DOI: 10.1002/ejic.200900329

Structure and Magnetic Properties of a New 1D Nickel(II) Hydroxythiophenedicarboxylate

Aude Demessence,[a][‡] Adel Mesbah,[b] Michel François,*[b] Guillaume Rogez,[a] and Pierre Rabu*[a]

Keywords: Nickel / Chain structures / Metal–organic frameworks / Magnetic properties

The new carboxylato-bridged Ni^{II} network $\{Ni_3(\mu_3\text{-}OH)_2[(\kappa^1\text{-}\kappa^1)\text{-}(\kappa^1\text{-}\kappa^1)\text{-}\mu_4 tdc]_2(H_2O)_4\}_n$ (H_2tdc = 2,5-thiophenedicarboxylic acid) has been synthesized hydrothermally. The structure has been characterized by synchrotron powder X-ray diffraction, thermogravimetric analysis, IR and UV/Vis spectroscopy. The title compound consists of $[Ni1O_6]_2[Ni2O_6]$ chains built of two edge-sharing octahedrons "$Ni1O_6$" linked via μ_3-OH to a vertex of the Ni2 octahedron. The connection between the chains is settled by the tdc^{2-} anions, leading to a 3D framework. The title compound exhibits a metamagnetic transition (T_N = 3.0 K, $\mu_0 H_C$ = 0.13 T at 1.8 K). This behaviour results from chains of ferromagnetic dimers coupled antiferromagnetically with intermediate Ni2, the competing set of interactions leading to a resultant moment. At low temperature, a 3D antiferromagnetic ordering occurs between the chains. The magnetic Ni–Ni interactions were evaluated by numerical resolution of the corresponding spin Hamiltonian. The structural and magnetic properties were compared with those of compounds exhibiting similar structural features and based on fumarate (fum^{2-}), terephthalate (tp^{2-}) and 1,4-cyclohexanedicarboxylate ($chdc^{2-}$).

Introduction

The synthesis and study of coordination polymers and metal–organic frameworks (MOFs) are one of the very active fields in materials chemistry and physics. These compounds associate an inorganic component (single ion or polynuclear cluster) and an organic ligand, which play the role of connectors and linkers, respectively. A huge variety of structures can be obtained, depending on the respective connectivity, charge, geometry of the connectors and linkers, the nature of the coordinating sites (carboxylic acid, amines, cyanides, polypyridines. ...) and the length of the linkers, as well as the presence of structuring agents, templates, capping ligands or counterions.[1–3]

Among the various types of ligands (or linkers) used to design MOFs, carboxylates are particularly well-placed, because of their robustness and the relatively easy access to functional molecules bearing carboxylate groups. Taking advantage of the combination of the properties of the building blocks, various (multi)functional carboxylate-based coordination polymers have been designed,[1,2,4–6] with applications in areas such as porosity for gas storage and separation,[7–13] catalysis,[14] ion sensing,[15] luminescence[16,17] and magnetism.[18,19] In relation with the present work, nickel-based coordination polymers including MOFs have been under focus in very recent reports.[20–23]

Monothiophenecarboxylates are particularly used in material sciences for their aromaticity. In the field of luminescent materials, they are interesting because of their ability to absorb and to transfer efficiently the energy of the π, π* excited state to rare earth ions to increase their luminescence quantum yield.[24–28] Thiophenecarboxylates have also been extensively employed to obtain transition-metal coordination complexes.[29–36] However, rather few magnetic studies have been reported.[37–42]

Continuing our research on the grafting of thiophenecarboxylates into layered magnetic transition-metal hydroxides,[43] we have extended our approach to the direct synthesis of polymeric magnetic networks incorporating the tdc^{2-} ligand (H_2tdc = 2,5-thiophenedicarboxylic acid, Scheme 1).

We have recently reported the synthesis, structure, and properties of a new Co^{II} thiophenedicarboxylate coordination polymer in which the tdc^{2-} ligand showed the unprecedented asymmetric tetradentate $(\kappa^1\text{-}\kappa^1)\text{-}(\kappa^1\text{-}\mu_2)\text{-}\mu_4$ coordination mode.[44]

[a] Institut de Physique et Chimie des Matériaux de Strasbourg, UMR 7504 CNRS – Université Louis Pasteur, Groupe des Matériaux Inorganiques,
23 rue du Loess, B. P. 43, 67034 Strasbourg cedex 2, France
Fax: +33-3-88107247
E-mail: Pierre.Rabu@ipcms.u-strasbg.fr
[b] Institut Jean Lamour, UMR 7198 CNRS – Nancy Université, rue du jardin botanique, B. P. 239, 54506 Vandœuvre lès Nancy, France
Fax: +33-3-83684611
E-mail: Michel.Francois@lcsm.uhp-nancy.fr
[‡] Present address: Institut Lavoisier, Université de Versailles St-Quentin-en-Yvelines,
45 avenue des Etats-Unis, 78035 Versailles Cedex, France

Supporting information for this article is available on the WWW under http://dx.doi.org/10.1002/ejic.200900329.

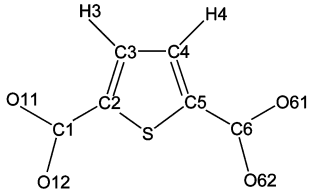

Scheme 1. The tdc^{2-} molecule with atom labelling.

We describe in this paper the hydrothermal synthesis, synchrotron powder X-ray diffraction structure, and magnetic properties of a new Ni^{II}(tdc) metal–organic framework. The structural and magnetic properties are compared with those of compounds with similar structural features based on fumarate (fum^{2-}),[45,46] terephthalate (tp^{2-})[47] and 1,4-cyclohexanedicarboxylate ($chdc^{2-}$).[48,49]

Results and Discussion

Synthesis

The synthesis was carried out under conditions slightly different from those used for the synthesis of the previously reported Co–tdc compound $\{Co[(\kappa^1\text{-}\kappa^1)\text{-}(\kappa^1\text{-}\mu_2)\text{-}\mu_4tdc](\mu_2\text{-}H_2O)_{0.5}(H_2O)\}_n$.[44] In particular, the quantity of base was smaller (1.4 equiv. for **1**, 2 equiv. for the Co compound). The reaction time was also longer for **1** (61 h) than for Co–tdc (22 h). Nevertheless, despite many attempts under different experimental conditions, no other Ni–tdc compound could be obtained but **1**.

Spectroscopy

Compound **1** was investigated by FTIR spectroscopy (Figure 1). In the high-frequency region, the main difference between the spectrum of **1** and the spectrum of the sodium salt of the ligand (Na_2tdc) corresponds to the presence of hydroxy groups and hydrogen-bonded water molecules in **1**. The spectrum of **1** indeed shows an intense and thin band at 3605 cm^{-1}, which can be attributed to the elongation of the hydroxy group.[50] The two bands at 3430 and 3250 cm^{-1} may be attributed to the antisymmetrical and symmetrical elongation modes of coordination water molecules implicated in hydrogen bonds. The shoulder at 3160 cm^{-1} is attributed to C–H elongation vibrations.

In the 1350–1700 cm^{-1} range, the frequencies of the antisymmetrical and symmetrical elongation modes for the carboxylate groups were found at $\nu(COO_{asym})$ = 1570 cm^{-1} and $\nu(COO_{sym})$ = 1385 cm^{-1}. The difference between the two characteristic bands is almost identical in **1** and in Na_2tdc ($\Delta\nu$ = 185 and 175 cm^{-1}, respectively), indicating a bidentate coordination mode of both carboxylate groups of the tdc^{2-} moieties, which agrees with the crystallographic structure.[51,52]

The UV/Vis/NIR spectrum shown in Figure 2 was recorded in the reflection mode and shows clearly three transition bands at ν_1 = 8800 cm^{-1} ($^3A_{2g}\rightarrow{}^3T_{2g}$), ν_2 = 15000 cm^{-1} ($^3A_{2g}\rightarrow{}^3T_{1g}$) and ν_3 = 26000 cm^{-1} [$^3A_{2g}\rightarrow{}^3T_{1g}$(P)]. The corresponding crystal field and Racah's parameter are $10Dq$ = 8880 cm^{-1} and B = 950 cm^{-1}, in accordance with values reported in the literature for octahedral Ni^{II} compounds.[53]

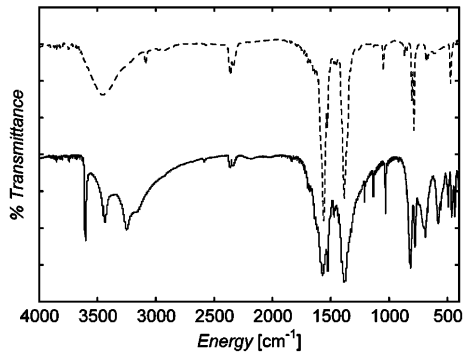

Figure 1. Infrared spectra of Na_2tdc (dashed line) and **1** (solid line).

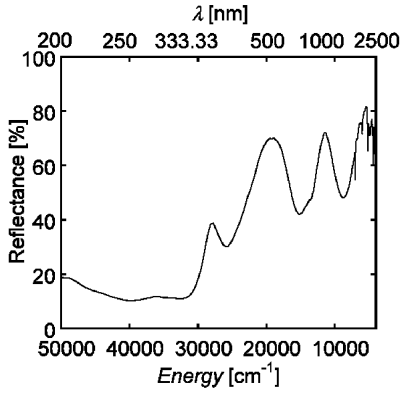

Figure 2. UV/Vis/NIR spectrum of **1**.

Thermal Analysis

Thermogravimetric analysis (TGA) for **1** reveals three successive weight losses in the temperature range 30–650 °C (Figure 3). The first two, between 100 and 280 °C, are related to the dissociation of coordinated water molecules and to dehydroxylation (obsd. 15%; calcd. 17.0%). The third

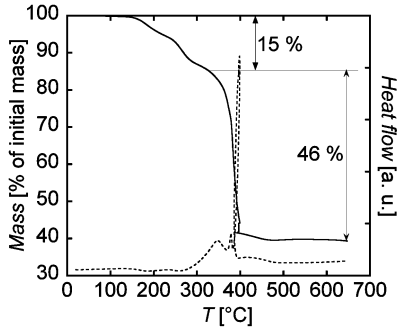

Figure 3. Thermogravimetric (solid line) and thermodifferential (dashed line) curves for **1**.

one, from 280 to 500 °C, corresponds to the exothermic dissociation and combustion of the tdc moiety and formation of the nickel oxide NiO (the nature of which was checked by powder X-ray diffraction) (obsd. 46%; calcd. 46.4%).

Structural Description

The structure of $\{Ni_3(\mu_3\text{-}OH)_2[(\kappa^1\text{-}\kappa^1)\text{-}(\kappa^1\text{-}\kappa^1)\text{-}\mu_4tdc]_2\text{-}(H_2O)_4\}_n$ (**1**) is shown in Figure 4, and selected interatomic distances and angles are reported in Table 5 (see Experimental Section). In this compound, the tdc^{2-} ligand exhibits a symmetrical tetradentate $(\kappa^1\text{-}\kappa^1)\text{-}(\kappa^1\text{-}\kappa^1)\text{-}\mu_4$ coordination mode. The structure is formed by chains (Figure 5) of nickel octahedra running parallel to the *a* axis and bridged by the bis(bidentate) tdc^{2-} anions. The connections between chains lead to a 3D framework (Figures 4a and b).

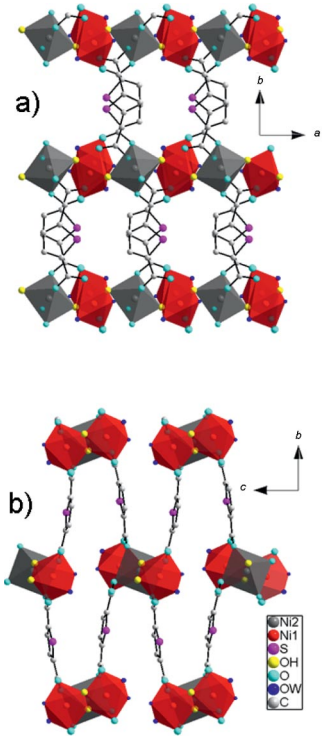

Figure 4. (a) View of the structure of **1** along the *c* axis. (b) View of the structure of **1** along the *a* axis.

The repeating structural unit in the nickel oxide chains is the $[Ni1O_6]_2[Ni2O_6]$ fragment formed by two edge-sharing $[Ni1O_6]$ octahedra related by the inversion centre and linked via μ_3-OH to a vertex of a $[Ni2O_6]$ octahedron. The coordination of Ni1 is ensured by the oxygen atoms of two water molecules, two μ_3-OH and two oxygen atoms from two carboxylate groups. The Ni2 coordination sphere is made of two μ_3-OH and four oxygen atoms belonging to four different carboxylate groups. The metal–oxygen distances Ni–O_H, Ni–O_{carb} and Ni–O_W range from 2.000(7) to 2.093(7) Å [av. 2.057(7) Å], 2.024(8) to 2.113(8) Å [av. 2.077(8) Å] and 2.097(7) to 2.187(8) Å [av. 2.142(8) Å], respectively. Thus it can be emphasized that the average distances are shorter for Ni–O_H, longer for Ni–O_W and intermediate for Ni–O_{carb}, in agreement with single-crystal X-ray diffraction data of the fumarate analogue **2**.[45]

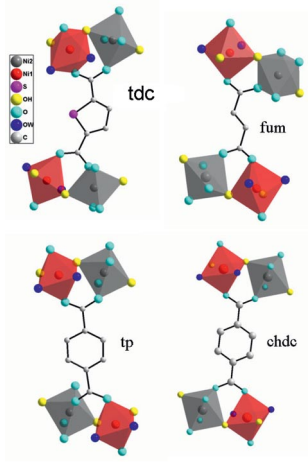

Figure 5. Representation of the connection between chains of "NiO_6" octahedra in the dicarboxylate ligands described in the text.

Comparative Structural Study

It is interesting to compare the structural properties of **1** with those of **2**,[45,46] **3**[47] and **4**,[48,49] which exhibit very similar Ni^{II} chain units interconnected by fumarate (fum^{2-}), terephthalate (tp^{2-}) and 1,4-cyclohexanedicarboxylate ($chdc^{2-}$), respectively.

First, the formula of **1** deduced from the powder X-ray structure analysis and the TGA experiment do not show the presence of solvated water, in contrast to what has been obtained for compounds **2** and **4**, based on fum^{2-} and $chdc^{2-}$, respectively. For the tp^{2-} compound **3**, the presence of solvated water molecules was less clear. For **1**, the analysis of the Fourier differences after the final Rietveld refinement does not show residual electronic density that could be attributed to water molecules. The presence of thiophene rings probably makes the "pores" of the structure hydrophobic.

The four compounds are built of the same $[Ni1O_6]_2[Ni2O_6]$ trimeric unit. Due to the connection mode of the organic ligands, the structures based on fum^{2-}, tdc^{2-} and $chdc^{2-}$ are 3D, while the one with tp^{2-} anions is 2D.[47] In the 3D structures, each chain is connected to four others by carboxylates with strong bonding, whereas in the 2D structure, each chain is connected to only two others by bis(bidentate) tp^{2-} anions.

Intrachain Ni–Ni distances and angles in the compounds based on tdc^{2-}, fum^{2-}, tp^{2-} and $chdc^{2-}$ are reported in Table 1 for comparison. The same nomenclature is used for the labelling of the Ni atoms in the four compounds (Ni1 lies in the general site, while Ni2 lies on a symmetry centre) and this system does not necessarily follow that of the original papers.

Table 1. Intrachain Ni–Ni distances [Å] and selected angles [°] in $Ni_3(OH)_2(di\text{-}carb)_2(H_2O)_4$ [di-carb^{2-}: tdc^{2-} in **1**, fum^{2-} in **2**, tp^{2-} in **3** and chdc^{2-} in **4**].

	1[a]	**2**[46]	**3**[47]	**4**[48,49]
Ni1–Ni1	3.045(2)	3.02	3.04	3.023
Ni1–Ni2	3.520(2), 3.498(2)	3.56, 3.66	3.55, 3.50	3.527, 3.527
Ni1–OH–Ni1	97.8(3)	94.23	99.4	95.78
Ni1–OH–Ni2	116.8(3), 117.4(3)	123.97, 120.08	123.0, 118.0	120.1, 120.1

[a] This work.

Concerning the distances between the Ni^{2+} magnetic centres, the Ni1–Ni1 values within the dimeric units are similar in the whole series and lie between 3.02 Å and 3.045 Å. As for the interdimer bridge, the values in **1** are almost equivalent to those found in **3** and **4** (Ni1–Ni2 3.50–3.52 Å) but differ significantly from those in **2** (3.56–3.66 Å), which exhibits a less symmetrical situation. Concerning the angles, Ni1–OH–Ni1 is slightly greater than 90° in all compounds, the highest values being measured in **1** and **3**, and Ni1–OH–Ni2 exceeds 116°.

The interchain distances between Ni atoms connected by the different dicarboxylate moieties are given in Table 2 for the four compounds and are illustrated in Figure 5 [$Ni1O_6$ (red) and $Ni2O_6$ (medium grey)]. These distances lie in the range 9.6–11.4 Å in **1**, **3**, **4** and are smaller in **2** (8.1–9.6 Å). The tetradentate $(\kappa^1\text{-}\kappa^1)\text{-}(\kappa^1\text{-}\kappa^1)\text{-}\mu_4$ coordination mode of the tdc^{2-} ligand in the present compound is one of the most often encountered for tdc^{2-}-based coordination compounds.[7,9,32,44] In the four compounds, interchain distances are large; hence, weak through-space interactions are expected.

Table 2. Interchain distances between Ni atoms [Å] in $Ni_3(OH)_2(di\text{-}carb)_2(H_2O)_4$ [di-carb^{2-}: tdc^{2-} in **1**, fum^{2-} in **2**, tp^{2-} in **3** and chdc^{2-} in **4**].

	1[a]	**2**[46]	**3**[47]	**4**[48,49]
Ni2–Ni2	10.34	8.754	10.20	11.22
Ni1–Ni1	9.614	9.651	11.31	11.38
Ni1–Ni2	10.83	8.140	10.30	10.74
Ni2–Ni1	9.892	8.832	10.52	10.74

[a] This work.

Interchain interactions could also arise from hydrogen-bond networks. The coordinates of the H atoms are reported in Table S1 (Supporting Information), and the hydrogen bond analysis is reported in Table 3. It appears from the DFT calculations that the orientation of the water molecules OW1 and OW2 leads to intrachain hydrogen bonds only. Indeed, hydrogen bonds are established between H atoms of water molecules OW1 and OW2 and O atoms of tdc^{2-} as shown by the H···A distances (H11···O62 1.685 and H21···O11 1.813 Å) and by the D–H···A angles close to 180°(see Figure 6). The H atom positions suggest that hydrogen bonds occur only inside the chains (intra) and not between the chains (inter) as illustrated in Figure 4. Actually, the result could be surprising, as the donor–acceptor O–O interchain distances are in the typical range for hydrogen bonds (2.726 Å). The lack of precise experimental localization of the H atoms by using powder X-ray diffraction makes it difficult to reach any definite conclusion. Yet, these features suggest that interchain interactions allowing 3D order (see later) are mainly driven by the tdc ligands.

Table 3. Hydrogen bonds in **1**.

D–H···A	*d*(D–H)	*d*(H···A)	*d*(D···A)	∠(D–H···A)	
OW1–H11···O62	1.00	1.68	2.67	167	Intrachain
OW2–H21···O11	1.00	1.81	2.80	168	Intrachain
OW1–OW2			2.72		no h.b.

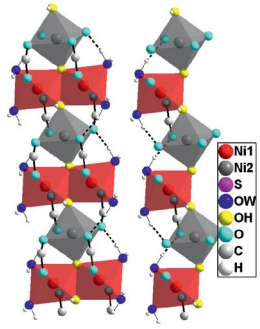

Figure 6. Partial view of **1** showing the intrachain hydrogen bonds (dashed lines).

Although the compounds based on tdc^{2-} and fum^{2-} have the same symmetry ($P2_1/c$) and the same orientation [100] for the chains and consequently a nearly identical *a* parameter (6.323 and 6.558 Å in **1** and **2**, respectively), their monoclinic axes are not comparable (the *b* and *c* axes are inverted and *c* in **1** plays the role of the *b* axis in **2**).

Magnetic Properties

The magnetic behaviour of **1** is presented in Figure 7. The molar susceptibility increases regularly with cooling and exhibits a sharp maximum of 1.68 K emu K mol^{-1} at 2.99 K followed by a steep decrease at lower temperatures. The variation of the χT product reveals a complex behaviour. The high-temperature value is consistent with the presence of three Ni^{II} ions per formula unit. Above 150 K, the susceptibility fits well the Curie–Weiss law with C = 3.73 emu K mol^{-1} corresponding to three S = 1 spin moments with an average g value of 2.25. A positive Weiss temperature, θ = +6.7 K, was also deduced in accordance with the increase in χT reaching a first rounded maximum of 4.14 emu K mol^{-1} at 36 K. Then a minimum is observed at 10 K preceding an abrupt upturn to a sharp maximum of 5.04 emu K mol^{-1} at T_N = 3.0 K.

Above T_N, the magnetization vs. field curve shown in Figure 8 at T = 4 K is typical of a paramagnet, whereas below the critical temperature, a metamagnetic transition is

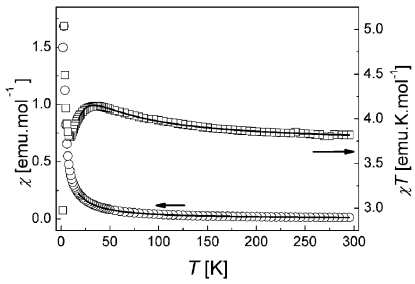

Figure 7. Thermal variation of the magnetic susceptibility of **1** under an applied field of 500 Oe. The full line corresponds to the best fit described in the text.

observed with a threshold field of $\mu_0 H_C$ = 0.13 T. This indicates the occurrence of a three-dimensional ordering consisting of two ferromagnetic-like subnetworks coupled antiferromagnetically with each other. It is worth noticing that the saturation value, Ms = 4.3 μ_B, is below that expected for three S = 1 spin moments (ca. 6.75 μ_B for g = 2.25). This is in favour of a ferrimagnetic ordering. In both regimes, just above and below T_N, a very small hysteresis was observed in the field region of the maximum curvature of the $M(H)$ curves. However, it is completely reversible at low field. This could be related to field-induced admixture between the low-lying spin states or a phonon bottleneck phenomenon.[54,55]

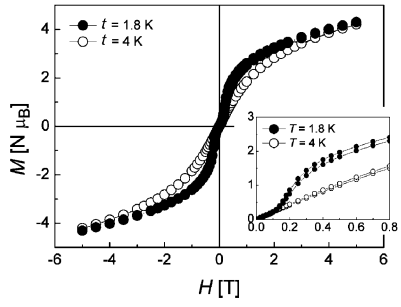

Figure 8. Magnetization vs. field curves for compound **1** at 4 K (open circles) and 1.8 K (filled circles). The inset is a zoom of the low-field region.

According to the structural features, the magnetic behaviour is mainly driven by that of the Ni^{II} chains running along the a axis, in which the Ni^{II} atoms can interact through efficient hydroxido bridges. Two exchange pathways can be identified in Figure 6, one within the Ni1 dimers (J_1) and the other between the Ni2 and the four adjacent Ni1 (J_2). No analytical expression is available for such a Heisenberg S = 1 spin system. Thus we have used a numerical model of Heisenberg S = 1 chains to evaluate the exchange interactions. Taking into account two different interactions and ruling out the border effect, calculations were done on the basis of closed rings of 3N spins arranged in interconnected butterfly motifs as shown in Scheme 2.

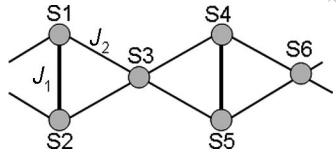

Scheme 2. Interaction scheme considered for the chain model used for fitting the experimental magnetic susceptibility of **1**. The closed ring consists of six spins (S1–S6) connected by two different interactions (J_1, J_2). The spin moments S1, S2, S4, S5 hold for Ni1 sites; S3 and S6 correspond to Ni2.

The corresponding spin Hamiltonian ($H = -\Sigma J_k S_i S_j$) was solved numerically up to N = 2 (i.e. six spins).[56] As shown in Figure 7, this model fits the experimental data well above 18 K; the best refined values are J_1 = +25.6(9) K, J_2 = –1.84(3) K, and the overall g value is 2.227(1). The same values lead to an upturn of the χT product below 10 K, suggesting a magnetic ground state, but it was not possible to fit very well the experimental divergence. This is likely due to the limited number of spins used for the calculation because of computer time limitation. Indeed, the low-temperature behaviour results from the divergence of the correlation length within the chains that our model based on short finite closed rings is not able to describe well.

Nevertheless, the general behaviour can be understood as resulting from chains of ferromagnetic Ni1 dimers coupling antiferromagnetically with intermediate Ni2, the competing set of interactions leading to a neat moment. It is consistent with the qualitative analysis suggested in previous studies on the parent compounds **2** and **4**.[45,46,48,49] Within the dimers, the Ni1 atoms are in edge-sharing oxygen octahedra with a Ni–O–Ni angle not very far from 90°, suggesting a significant ferromagnetic contribution to the exchange coupling. On the other hand, the Ni1–Ni2 interaction occurring between corner-sharing octahedra with large metal–oxygen–metal angles is expected to be weaker and antiferromagnetic.[57,58] The quantitative result reported here for compound **1** is consistent with this analysis, showing that J_1 is ferromagnetic and an order of magnitude larger than the antiferromagnetic J_2. This leads to a ferrimagnetic arrangement of the spin moments along the chains, pointing in one direction on the Ni1 sites and in the opposite direction on Ni2 with a 2:1 multiplicity. At low temperature, a 3D antiferromagnetic ordering occurs between the chains through the thiophene dicarboxylates along b. Such an antiferromagnetic ground state was not observed in the analogous compounds **2** and **4**, which are reported to behave as ferrimagnets within the same temperature range, indicating that the nature of the bridging ligand is not innocent. It is worth noticing that the terephthalate compound **3** was reported by some of the authors to exhibit an increase in the χT product when cooling down to 4.2 K, indicating a regular ferromagnetic behaviour although consisting of similar nickel chains. This could be related either to the influence of the bridging ligand or to some water loss that can induce a ferrimagnetic-to-ferromagnetic transition as

explained for compound **4**.[48,49] Further experiments on the terephthalate compound are under way, especially magnetic measurements at lower temperatures.

Conclusions

The new carboxylato-bridged Ni^{II} compound $\{Ni_3(\mu_3\text{-}OH)_2[(\kappa^1\text{-}\kappa^1)\text{-}(\kappa^1\text{-}\kappa^1)\text{-}\mu_4tdc]_2(H_2O)_4\}_n$ (H_2tdc = 2,5-thiophenedicarboxylic acid) has been synthesized by using a hydrothermal route and fully characterized by ancillary techniques. The structure has been solved ab initio from synchrotron powder X-ray diffraction. It consists of stacked Ni^{II} chains with butterfly motifs built from two edge-sharing octahedra "Ni1O_6" linked via μ_3-OH to a vertex of the Ni2 octahedron. The chains are interconnected by the tdc^{2-} anions, which leads to a 3D framework. The title compound shows a metamagnetic transition (T_N = 3.0 K, $\mu_0 H_C$ = 0.13 T at 1.8 K). This behaviour results from antiferromagnetic coupling between ferrimagnetic chains. The numerical fit of the magnetic susceptibility data indicates a ferromagnetic coupling within the Ni1 dimer units and a much weaker antiferromagnetic coupling with Ni2. This is consistent with previous results on fumarate (**2**) and 1,4-cyclohexanedicarboxylate (**4**) analogues whose behaviours were analyzed only qualitatively. In this series, the fact that a 3D antiferromagnetic or ferromagnetic ordering occurs between the chains at low temperature bears out that connecting the chains with different ligands involving π electrons can tune the magnetic interactions, still at quite large distances.[59–61]

Experimental Section

Materials: All chemicals were obtained from Aldrich and used as received without further purification. Elemental analyses for C, H and S were carried out by the Analytical Department at the Institut Charles Sadron (Strasbourg, France). The amount of nickel was evaluated by thermogravimetric analysis (see below).

$[Ni_3(\mu_3\text{-}OH)_2[(\kappa^1\text{-}\kappa^1)\text{-}(\kappa^1\text{-}\kappa^1)\text{-}\mu_4tdc]_2(H_2O)_4]$ (1): $Ni(H_2O)_6Cl_2$ (0.36 g, 1.5 mmol), 2,5-thiophenedicarboxylic acid (H_2tdc) (0.26 g, 1.5 mmol) and aqueous sodium hydroxide (0.2 mol/L, 10.5 mL, 2.1 mmol) were placed in a home-built, Teflon-lined, stainless steel pressure bomb of 75 mL maximum capacity. A stream of Ar was passed through the solution for 15 min, and then the bomb was sealed and heated at 180 °C for 61 h under autogenous pressure. After slow cooling to room temperature, the bomb was opened, and the microcrystalline light-green powder was filtered and washed with water and ethanol. Yield: 70%. $C_{12}H_{14}O_{14}S_2Ni_3$ (622.43): C 23.16, H 2.27, S 10.30, Ni 28.29; found C 23.81, H 2.36, S 9.62, Ni 26.71.

Physical Measurements: UV/Vis/NIR spectroscopic studies were performed with a Perkin–Elmer Lambda 19 instrument. The spectra were recorded by reflection with a resolution of 4 nm and a sampling rate of 240 nm min^{-1}. FTIR studies were carried out with a Digilab Excalibur 3000 computer-driven instrument on 0.1 mm thick powder samples in KBr. Thermogravimetric experiments were performed with a TA Instruments STD Q600 apparatus heating the sample in air from 20 to 700 °C at a rate of 5 °C min^{-1}. Magnetic data were collected with a Quantum Design MPMS-XL 5S SQUID magnetometer covering the temperature and field ranges 1.8–300 K, ±5 T. Data were corrected for the sample holder and diamagnetism was estimated from Pascal constants.

XRPD and Ab Initio Structure Determination

Powder X-ray diffraction (PXRD) data were collected at 100 K with synchrotron radiation at ESRF, on the beam line ID31 (λ = 0.851243 Å). The diffractometer was equipped with a primary Si(111) double crystal monochromator and nine sensitive linear position detectors coupled with crystal analyzers.[62] The fine powder of the title compound was introduced in a Lindemann tube (Φ = 0.8 mm), and data were measured by using transmission Debye–Scherrer geometry. Patterns were recorded for two hours in the range $3 < 2\theta < 43°$ with an interval of 0.01°. Crystal data and structure refinement parameters are reported in Table 4.

Table 4. Crystal data and Rietveld refinement parameters for **1**.

Compound	$Ni_3(OH)_2(O_2CC_4H_2SCO_2)_2(H_2O)_4$
Formula	$C_{12}H_{14}Ni_3O_{14}S_2$
Fw [g mol^{-1}]	622.44
System	monoclinic
Space group	$P2_1/c$
a [Å]	6.3232(1)
b [Å]	19.1075(2)
c [Å]	7.9305(1)
β [°]	96.373(1)
V [Å^3]	952.248(3)
Z	2
D_x [g cm^{-3}]	2.170
Wavelength [Å]	0.851243
Absorption coefficient ($\mu \times r$)	2.53
2θ range [°]	3–35
Observed points	13313
N_{ref}	643
R_p	0.091
R_{wp}	0.118
χ^2	7.27
R_{Bragg}	0.058
R_F	0.053
N profile parameters	19
N intensity-dependent parameters	57

Indexing: Standard peak search methods were used to locate the diffraction maxima with the Reflex program from Material Studio System Software (Accelrys).[63] The Xcell indexing program from Material Studio,[64] allowing space group determination, was used. The solution was found in $P2_1/c$ with the parameters a = 6.3233 Å, b = 19.1069 Å, c = 7.9313 Å, β = 96.38°, V = 952.32 Å^3 with a relative factor of merit for the 23 first reflections of 29.9. A Pawley fitting led to an R_p value of 0.07.

Resolution:[65] The structure was solved by direct methods with the EXPO2004 program.[66,67] For this purpose, a *hkl* file was created with the Fullprof program running in the "profile matching" mode for the Lebail decomposition.[68] To estimate accurately the integrated intensities, a resolution function was primarily obtained by measuring silicon from the National Bureau of Standards as a standard reference material. Then, the peak shape was described by using the Thomson–Cox–Hasting function (function 7 in Fullprof). An anisotropic peak broadening has been modelled by considering crystallite size and strain effects. The *hkl* file treated by EXPO2004 contained 643 independent reflections. No constrain was applied on atoms of the tdc^{2-} molecule, and an initial model was found, with the chemical formula $Ni_3(OH)_2(H_2O)_4(C_6H_2O_4S)_2$ (except for

the H atoms which were too light to be located), in agreement with the elemental analysis results for C, H, S and Ni. The asymmetric unit contains two sites for Ni, seven for O, six for C and one for S atoms. No additional O site attributable to a possible water molecule as solvent was detected. All the atoms lay in general positions except for Ni2, which was situated on the symmetry centre 2a. Preliminary refinement of the model converged to a confidence R_{Bragg} factor of 0.08.

Refinement of the structure was performed by the Rietveld method with the FULLPROF program.[68] The structure was refined to a final R_{Bragg} value of 0.058 without applying any constraint on the thiophene molecule. Nevertheless, the goodness of the data allowed retrieving realistic geometrical parameters for the molecule (see Table 5 and Scheme 1). Observed, calculated and difference patterns are shown in Figure 9. The fractional atomic coordinates can be found in the Supporting Information.

Table 5. Selected interatomic distances and angles in **1**.

Atom	Atom	Distance [Å]	Atom	Atom	Atom	Angle [°]
Ni1	O_W1	2.097(7)	C2	C1	O11	117.5(16)
	O_W2	2.187(8)	C2	C1	O12	120.7(16)
	OH	2.041(8)	C5	C8	O81	116.9(17)
	OH	2.000(7)	C5	C8	O82	115(2)
	O12	2.024(8)	C7	C2	C3	118.8(16)
	O61	2.078(8)	C2	C3	C4	120.8(9)
Ni2	OH	2.093(7)	C3	C4	C5	115.5(19)
	O62	2.067(8)	C4	C5	C6	126.2(17)
	O11	2.113(8)	C5	C6	C7	115(2)
S1	C2	1.725(14)	C6	C7	C2	122.2(18)
	C5	1.757(13)	C2	S1	C5	89.5(10)
C1	C2	1.499(19)	O11	C1	C2	114.0(15)
	O12	1.245(16)	C1	C2	S1	115.3(12)
	O11	1.287(15)	C1	C2	C3	129.9(17)
C2	C3	1.347(18)	O11	C1	O12	122.1(14)
C3	C4	1.436(16)	C2	C3	C4	111.8(16)
C4	C5	1.384(18)	C3	C4	C5	111.8(15)
C5	C6	1.480(19)	C4	C5	S1	112.1(12)
C6	O62	1.275(16)	S1	C5	C6	118.9(13)
C6	O61	1.245(16)	C4	C5	C6	128.9(17)
			O62	C6	O61	124.5(14)
			O62	C6	C5	116.3(14)
			O61	C6	C5	119.2(15)

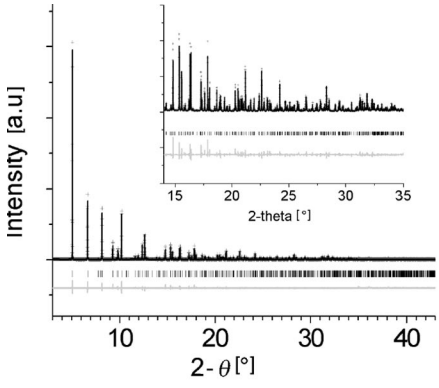

Figure 9. Observed (top), calculated (middle) and difference (bottom) XRPD patterns in **1** (λ = 0.851242 Å). The vertical bars indicate the Bragg positions.

The H atoms (seven H sites) were then positioned with the graphical facilities of MS Modeling, and their coordinates were refined with DFT methods by using the Dmol^3 program from Accelrys.[69,70] We used DFT Semi-core Pseudo Potentials (DSPP) with a double numerical plus d-functions (DND) basis set.[71] The exchange correlation was treated with the gradient-corrected PBE functional.[72] The Brillouin-zone integration was performed by using a $3 \times 2 \times 2$ grid, and the SCF (Self Consistent Field) convergence tolerance was 10^{-5}. For this purpose, the position of the non-hydrogen atoms was kept to the value refined before by the Rietveld method. Atomic positions of H atoms are reported in Table S1. (The statistical factors of the Rietveld refinement reported in Table 1 are for a model which does not take into account the H atoms.)

Supporting Information (see footnote on the first page of this article): Table of the fractional atomic coordinates.

Acknowledgments

We thank D. Burger for TGA measurements and Irena Margiolaki from the "European Synchrotron Radiation Facilities (ESRF)" in Grenoble, France, for helping us in our experiments. We thank the CNRS, the Université Henri Poincaré de Nancy and the Université Louis Pasteur de Strasbourg for support. G. R. is grateful to the Agence Nationale de la Recherche for financial support (ANR contract ANR-06-JCJC-0008). A. D. thanks the French Ministry for Education, Research and Technology for her PhD grant.

[1] S. Kitagawa, R. Kitaura, S.-i. Noro, *Angew. Chem. Int. Ed.* **2004**, *43*, 2334–2375.
[2] D. Maspoch, D. Ruiz-Molina, J. Veciana, *Chem. Soc. Rev.* **2007**, *36*, 770–818.
[3] C. N. R. Rao, S. Natarajan, R. Vaidhyanathan, *Angew. Chem. Int. Ed.* **2004**, *43*, 1466–1496.
[4] G. Ferey, C. Mellot-Draznieks, C. Serre, F. Millange, *Acc. Chem. Res.* **2005**, *38*, 217–225.
[5] D. Bradshaw, J. B. Claridge, E. J. Cussen, T. J. Prior, M. J. Rosseinsky, *Acc. Chem. Res.* **2005**, *38*, 273–282.
[6] C. Janiak, *Dalton Trans.* **2003**, 2781–2804.
[7] N. L. Rosi, J. Kim, M. Eddaoudi, B. Chen, M. O'Keeffe, O. M. Yaghi, *J. Am. Chem. Soc.* **2005**, *127*, 1504–1518.
[8] M. Eddaoudi, J. Kim, N. Rosi, D. Vodak, J. Wachter, M. O'Keeffe, O. M. Yaghi, *Science* **2002**, *295*, 469–472.
[9] M. Eddaoudi, J. Kim, D. Vodak, A. Sudik, J. Wachter, M. O'Keeffe, O. M. Yaghi, *Proc. Natl. Acad. Sci. USA* **2002**, *99*, 4900–4904.
[10] M. Eddaoudi, D. B. Moler, H. Li, B. Chen, T. M. Reineke, M. O'Keeffe, O. M. Yaghi, *Acc. Chem. Res.* **2001**, *34*, 319–330.
[11] J. L. C. Rowsell, O. M. Yaghi, *Angew. Chem. Int. Ed.* **2005**, *44*, 4670–4679.
[12] G. Férey, C. Mellot-Draznieks, C. Serre, F. Millange, J. Dutour, S. Surblé, I. Margiolaki, *Science* **2005**, *309*, 2040–2042.
[13] B. Chen, C. Liang, J. Yang, D. S. Contreras, Y. L. Clancy, E. B. Lobkovsky, O. M. Yaghi, S. Dai, *Angew. Chem. Int. Ed.* **2006**, *45*, 1390–1393.
[14] L. Pan, H. Liu, X. Lei, X. Huang, D. H. Olson, N. J. Turro, J. Li, *Angew. Chem. Int. Ed.* **2003**, *42*, 542–546.
[15] B. Chen, L. Wang, F. Zapata, G. Qian, E. B. Lobkovsky, *J. Am. Chem. Soc.* **2008**, *130*, 6718–6719.
[16] M. Xue, G. Zhu, Y. Li, X. Zhao, Z. Jin, E. Kang, S. Qiu, *Cryst. Growth Des.* **2008**, *8*, 2478–2483.
[17] L. Zhang, Y.-Y. Qin, Z.-J. Li, Q.-P. Lin, J.-K. Cheng, J. Zhang, Y.-G. Yao, *Inorg. Chem.* **2008**, *47*, 8286–8293.
[18] D. Maspoch, D. Ruiz-Molina, K. Wurst, N. Domingo, M. Cavallini, F. Biscarini, J. Tejada, C. Rovira, J. Veciana, *Nat. Mater.* **2003**, *2*, 190.
[19] H. O. Stumpf, Y. Pei, O. Kahn, L. Ouahab, D. Grandjean, *Science* **1993**, *261*, 447–449.

[20] J. Chakraborty, M. Nandi, H. Mayer-Figge, W. S. Sheldrick, L. Sorace, A. Bhaumik, P. Banerjee, *Eur. J. Inorg. Chem.* **2007**, 5033–5044.
[21] F. A. Cotton, C. A. Murillo, Q. Wang, M. D. Young, *Eur. J. Inorg. Chem.* **2008**, 5257–5262.
[22] H. A. Habib, J. Sanchiz, C. Janiak, *Dalton Trans.* **2008**, 4877–4884.
[23] S. Neogi, E. C. Sañudo, P. K. Bharadwaj, *Eur. J. Inorg. Chem.* **2007**, 5426–5432.
[24] E. E. S. Teotonio, M. C. F. C. Felinto, H. F. Brito, O. L. Malta, A. C. Trindade, R. Najjar, W. Strek, *Inorg. Chim. Acta* **2004**, *357*, 451.
[25] L. Yuan, M. Yin, E. Yuan, J. Sun, K. Zhang, *Inorg. Chim. Acta* **2004**, *357*, 89.
[26] L. Yuan, Z. Li, J. Sun, K. Zhang, *Spectrochim. Acta Part A* **2003**, *59*, 2949.
[27] M.-C. Yin, L.-J. Yuan, C.-C. Ai, C.-W. Wang, E. T. Yuan, J.-T. Sun, *Polyhedron* **2004**, *23*, 529.
[28] L.-Z. Cai, W.-T. Chen, M.-S. Wang, G.-C. Guo, J.-S. Huang, *Inorg. Chem. Commun.* **2004**, *7*, 611.
[29] M. J. Byrnes, M. H. Chisholm, *Chem. Commun.* **2002**, 2040–2041.
[30] M. J. Byrnes, M. H. Chisholm, R. J. H. Clark, J. C. Gallucci, C. M. Hadad, N. J. Patmore, *Inorg. Chem.* **2004**, *43*, 6334–6344.
[31] X.-Z. Sun, B.-H. Ye, *Acta Crystallogr., Sect. E* **2004**, *60*, m878.
[32] B.-L. Chen, K.-F. Mok, S.-C. Ng, M. G. B. Drew, *New J. Chem.* **1999**, *23*, 877–883.
[33] B. L. Chen, K. F. Mok, S.-C. Ng, Y.-L. Feng, S.-X. Liu, *Polyhedron* **1998**, *17*, 4237–4247.
[34] B.-L. Chen, K.-F. Mok, S.-C. Ng, M. G. B. Drew, *Polyhedron* **1999**, *18*, 1211–1220.
[35] P. Drożdżewski, A. Brożyna, M. Kubiak, *J. Mol. Struct.* **2004**, *707*, 131.
[36] M. V. Marinho, M. I. Yoshida, K. J. Guedes, K. Krambrock, A. J. Bortoluzzi, M. Horner, F. C. Machado, W. M. Teles, *Inorg. Chem.* **2004**, *43*, 1539–1544.
[37] H. W. Richardson, J. R. Wasson, W. E. Hatfield, *J. Mol. Struct.* **1977**, *36*, 83.
[38] F. Moro, V. Corradini, M. Evangelisti, V. D. Renzi, R. Biagi, U. d. Pennino, C. J. Milios, L. F. Jones, E. K. Brechin, *J. Phys. Chem. B* **2008**, *112*, 9729–9735.
[39] V. Tangoulis, D. Panagoulis, C. P. Raptopoulou, C. Dendrinou-Samara, *Dalton Trans.* **2008**, 1752–1760.
[40] J. J. Henderson, C. M. Ramsey, E. del Barco, A. Mishra, G. Christou, *J. Appl. Phys.* **2007**, *101*, 09E102.
[41] P. Kopel, Z. Trávníček, J. Marek, M. Korabik, J. Mrozinski, *Polyhedron* **2003**, *22*, 411.
[42] T. Kuroda-Sowa, T. Nogami, H. Konaka, M. Maekawa, M. Munakata, H. Miyasaka, M. Yamashita, *Polyhedron* **2003**, *22*, 1795.
[43] A. Demessence, G. Rogez, P. Rabu, *Chem. Mater.* **2006**, *18*, 3005–3015.
[44] A. Demessence, G. Rogez, R. Welter, P. Rabu, *Inorg. Chem.* **2007**, *46*, 3423–3425.
[45] S. Konar, P. S. Mukherjee, E. Zangrando, F. Lloret, N. R. Chaudhuri, *Angew. Chem. Int. Ed.* **2002**, *41*, 1561–1563.
[46] N. Guillou, S. Pastre, C. Livage, G. Ferey, *Chem. Commun.* **2002**, 2358–2359.
[47] A. Carton, A. Mesbah, T. Mazet, F. Porcher, M. Francois, *Sol. State Sci.* **2007**, *9*, 465.
[48] J. Chen, M. Ohba, D. Zhao, W. Kaneko, S. Kitagawa, *Cryst. Growth Des.* **2006**, *6*, 664–668.
[49] M. Kurmoo, H. Kumagai, M. Akita-Tanaka, K. Inoue, S. Takagi, *Inorg. Chem.* **2006**, *45*, 1627–1637.
[50] K. Nakamoto, *Infrared and Raman Spectra of Inorganic and Coordination Compounds*, Fourth Edition, Wiley Interscience, New York, **1986**.
[51] C. Dendrinou-Samara, G. Tsotsou, L. V. Ekateriniadou, A. H. Kortsaris, C. P. Raptopoulou, A. Terzis, D. A. Kyriakidis, D. P. Kessissoglou, *J. Inorg. Biochem.* **1998**, *71*, 171–179.
[52] G. B. Deacon, R. J. Phillips, *Coord. Chem. Rev.* **1980**, *33*, 227–250.
[53] A. B. P. Lever, *Inorganic Electronic Spectroscopy, 2nd Edition*, Elsevier, Amsterdam, **1984**, p. 479–505.
[54] D. Collison, M. Murrie, V. S. Oganesyan, S. Piligkos, N. R. J. Poolton, G. Rajaraman, G. M. Smith, A. J. Thomson, G. A. Timko, W. Wernsdorfer, R. E. P. Winpenny, E. J. L. McInnes, *Inorg. Chem.* **2003**, *42*, 5293–5303.
[55] I. Chiorescu, W. Wernsdorfer, A. Muller, H. Bogge, B. Barbara, *J. Magn. Magn. Mater.* **2000**, *221*, 103.
[56] P. Legoll, M. Drillon, P. Rabu, F. Maingot, SPINv.2.35 is a program for calculation and modeling of the magnetic properties of low-dimensional systems. It involves the diagonalization subroutine rsm for finding eigenvalues and vectors of symmetrical matrices, included in the FORTRAN library EISPACK, and the function minimization program MINUIT, CERN Program Library Entry D506, Geneva, Switzerland.
[57] J. Kanamori, *J. Phys. Chem. Solids* **1959**, *20*, 87–98.
[58] E. Ruiz, S. Alvarez, A. Rodriguez-Fortea, P. Alemany, Y. Pouillon, C. Massobrio in *Electronic Structure and Magnetic Behavior in Polynuclear Transition-Metal Compounds*, *Vol. II* (Eds.: J. S. Miller, M. Drillon), Wiley-VCH Verlag GmbH, Weinheim, Germany, **2001**, pp. 227–279.
[59] P. Rabu, M. Drillon, *Adv. Eng. Mater.* **2003**, *5*, 189–210.
[60] P. Rabu, J.-M. Rueff, Z.-L. Huang, S. Angelov, J. Souletie, M. Drillon, *Polyhedron* **2001**, *20*, 1677–1685.
[61] C. Hornick, P. Rabu, M. Drillon, *Polyhedron* **2000**, *19*, 259–266.
[62] A. N. Fitch, *J. Res. Natl. Inst. Stand. Technol.* **2004**, *109*, 133–142.
[63] http://www.accelrys.com/products/mstudio/modeling/crystallization/reflex.html.
[64] A. M. Neumann, *J. Appl. Crystallogr.* **2003**, *36*, 356–365.
[65] CCDC-716347 contains the supplementary crystallographic data for this paper. These data can be obtained free of charge from The Cambridge Crystallographic Data Centre via www.ccdc.cam.ac.uk/data_request/cif.
[66] A. Altomare, M. C. Burla, G. L. Cascarano, C. Giacovazzo, A. Guagliardi, A. G. G. Moliterni, G. Polidori, R. Rizzi, M. Camalli, *J. Appl. Crystallogr.* **1999**, *32*, 339–340.
[67] A. Altomare, R. Caliandro, M. Camalli, C. Cuocci, C. Giacovazzo, A. G. G. Moliterni, R. Rizzi, *J. Appl. Crystallogr.* **2004**, *37*, 1025–1028.
[68] J. Rodriguez-Carvajal, M. T. Fernandez-Diaz, J. L. Martinez, *J. Phys.: Cond. Mater.* **1991**, *3*, 3215–3234.
[69] B. Delley, *J. Phys. Chem.* **1996**, *100*, 6107–6110.
[70] B. Delley, *J. Phys. Chem.* **2006**, *110*, 13632–13639.
[71] B. Delley, *Phys. Rev. B* **2002**, *66*, 155125.
[72] J. P. Perdew, K. Burke, M. Ernzerhof, *Phys. Rev. Lett.* **1996**, *77*, 3865–3868.

Received: April 9, 2009
Published Online: July 24, 2009

